
Custom Focal Plane Arrays of SPADs

Erik K. Duerr¹, Anup Katake², Jason Mumolo²

The International SPAD Sensor Workshop 2020

9 June 2020



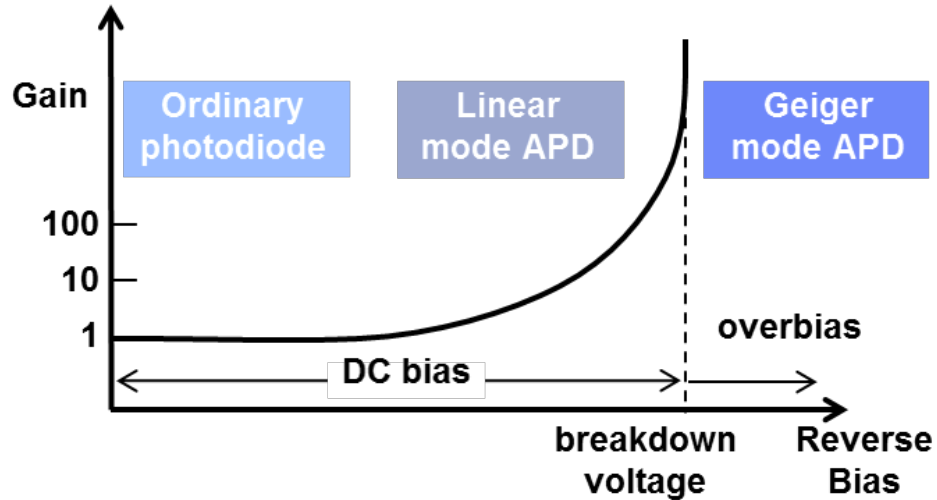
¹ Lincoln Laboratory, Massachusetts Institute of Technology

² Jet Propulsion Laboratory, California Institute of Technology



Geiger-Mode Avalanche Photodiode (GmAPD) Detector Technology

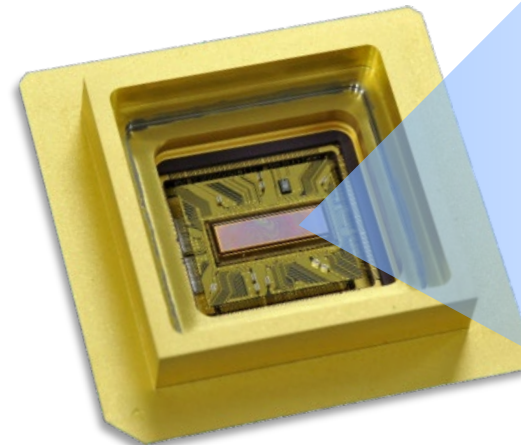
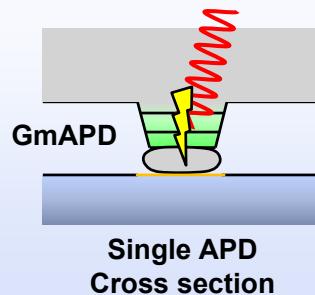
Photodiode Modes of Operation for MIT/LL Digital Pixel FPAs



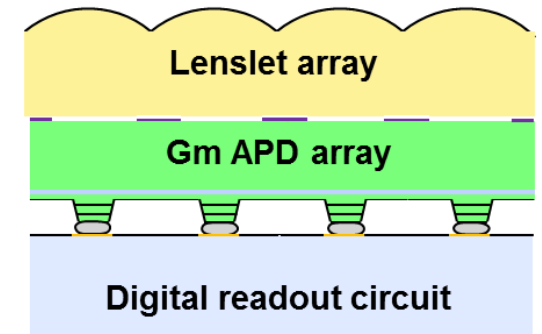
Geiger-mode APDs provide:

- Single-photon sensitivity
- Lots of current → easy digitization
- Fast breakdown → excellent (sub-ns) time resolution
- TEC accessible temperatures → low SWAP
- Large format arrays

A single photon absorbed by the overbiased APD generates a fast rush of current



Device Cross-section





AOSTB Ladar Hurricane Harvey Response

Unprecedented Harvey Damage



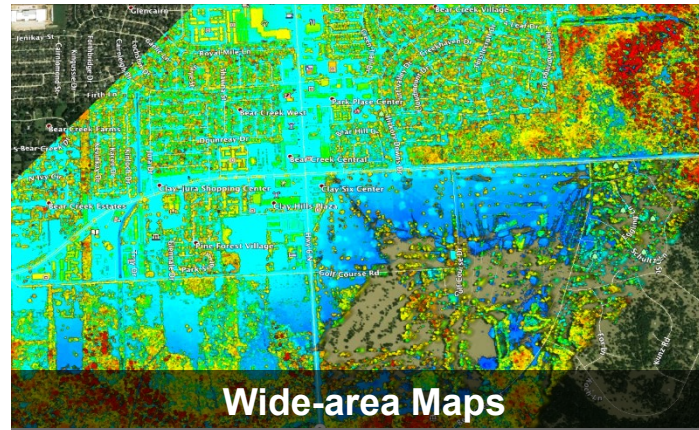
- 203,000 homes damaged
- 500,000 vehicles destroyed
- 200 million cubic yards of debris
- 30,000 people displaced
- 13 Superfund sites flooded



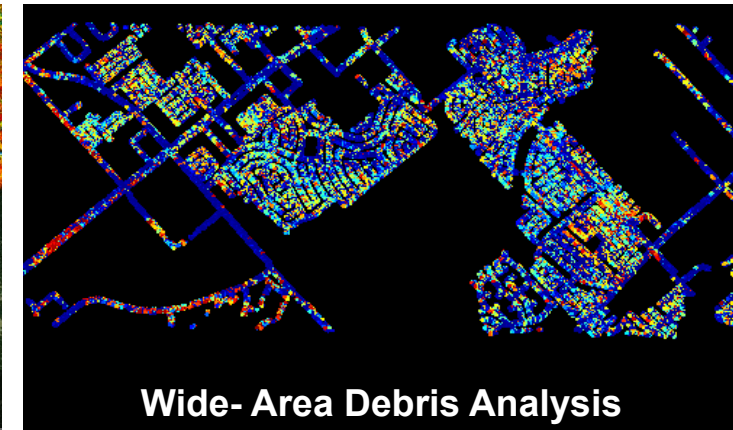
Urgent FEMA Requests

1. Wide-area debris mapping and quantification
2. Infrastructure damage assessment
3. Flood extent and volume

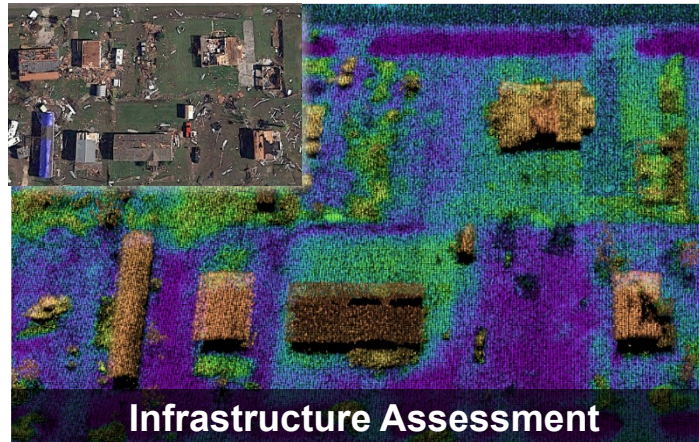
AOSTB Ladar responds to FEMA needs



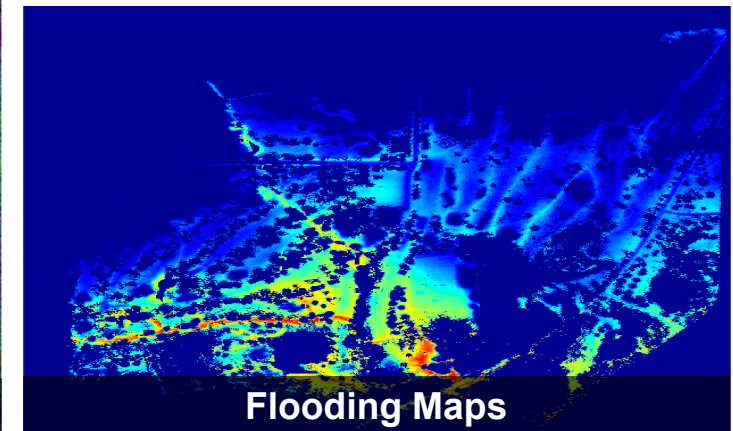
Wide-area Maps



Wide- Area Debris Analysis



Infrastructure Assessment



Flooding Maps

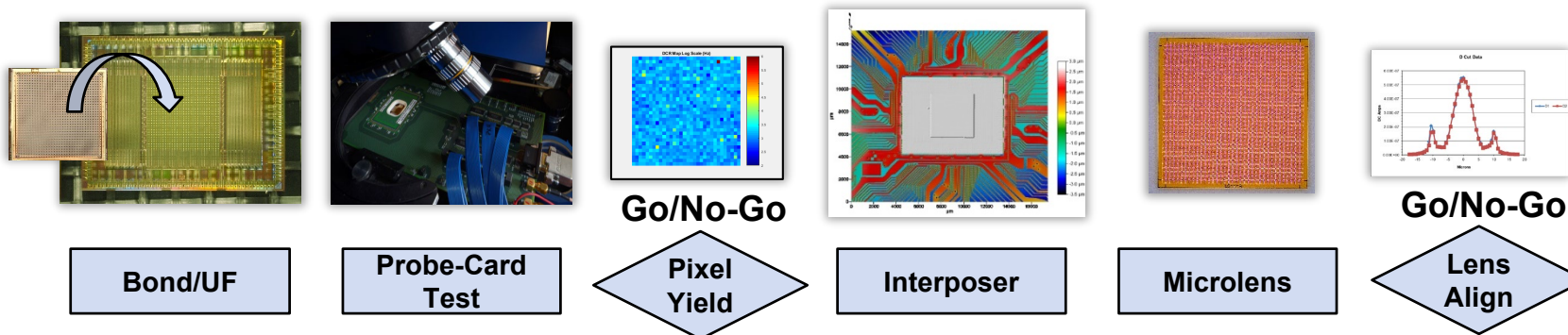
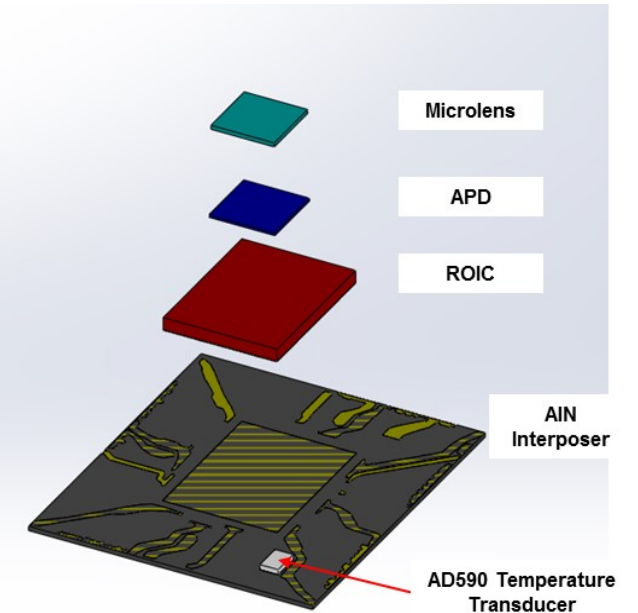
Advanced Ladar sensor potentially game-changing to recovery and public assistance efforts



Sensor Chip Assembly (SCA)

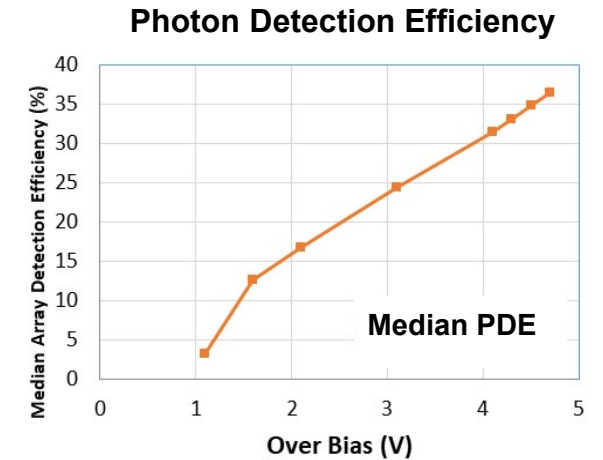
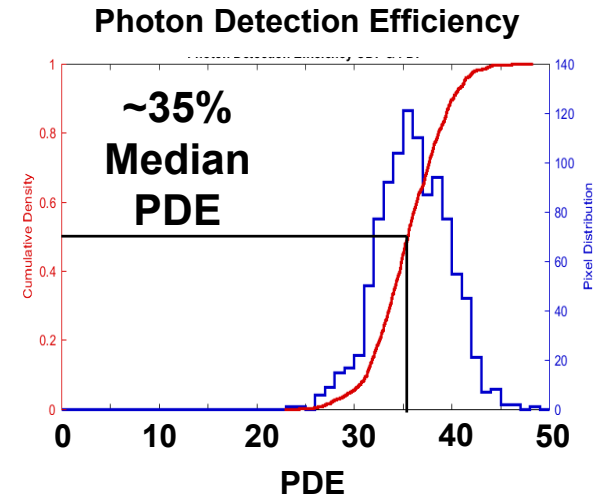
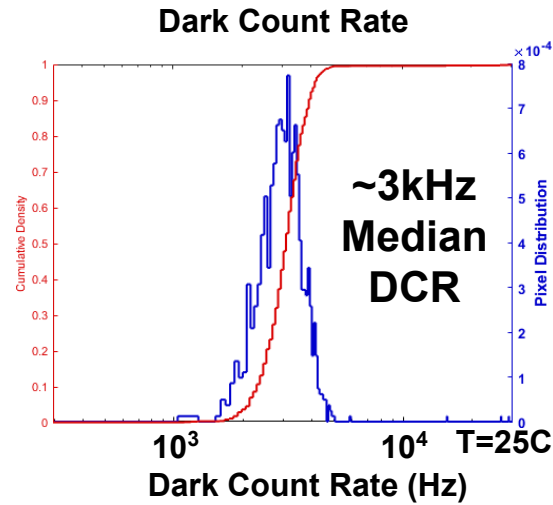
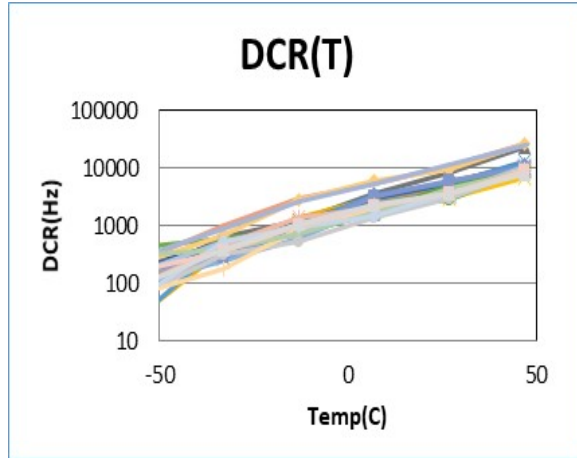
- InP/InGaAsP APD array bump bonded to ROIC with indium bumps
 - Probe-card testing and underfill after bump bonding APD to ROIC
- ROIC precision placed and epoxied on AlN interposer
- GaP microlens array actively aligned to APDs and attached with epoxy
 - ~0.5 μm accuracy
- Temperature sensor epoxied on interposer
 - Monitors SCA temperature

SCA Components





Typical InP-based Detector Performance

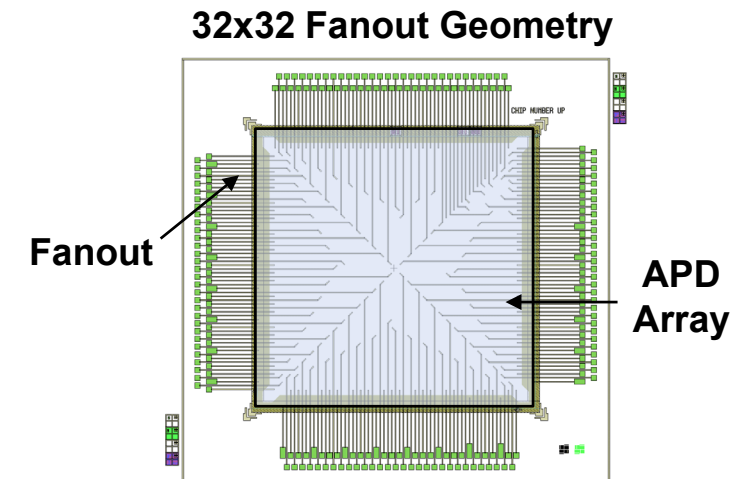
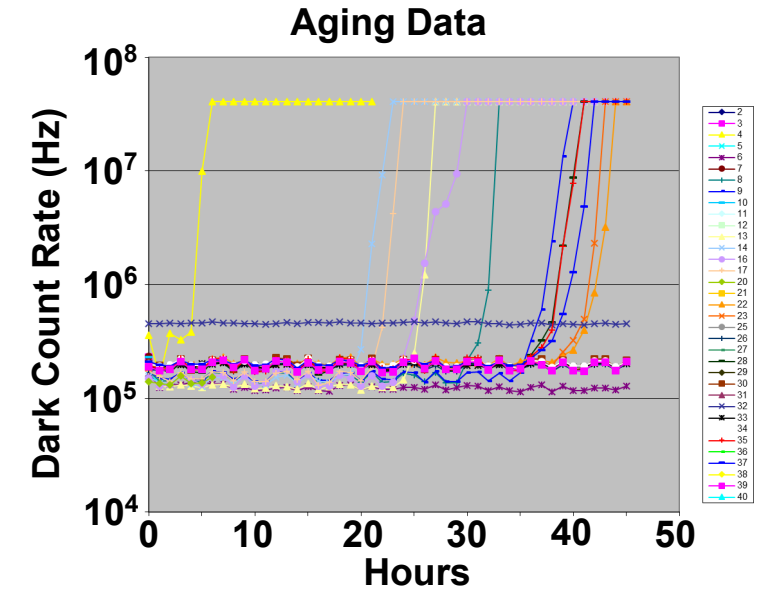


- **Median dark count rate ~3 kHz at room temperature (25 C)**
 - DCR varies in expected manner with temperature
- **PDE achieves > 30% PDE at >4 V overbias**
 - Readout integrated circuit can achieve overbias values up to ~6 V



InP-based Geiger-mode APD Reliability

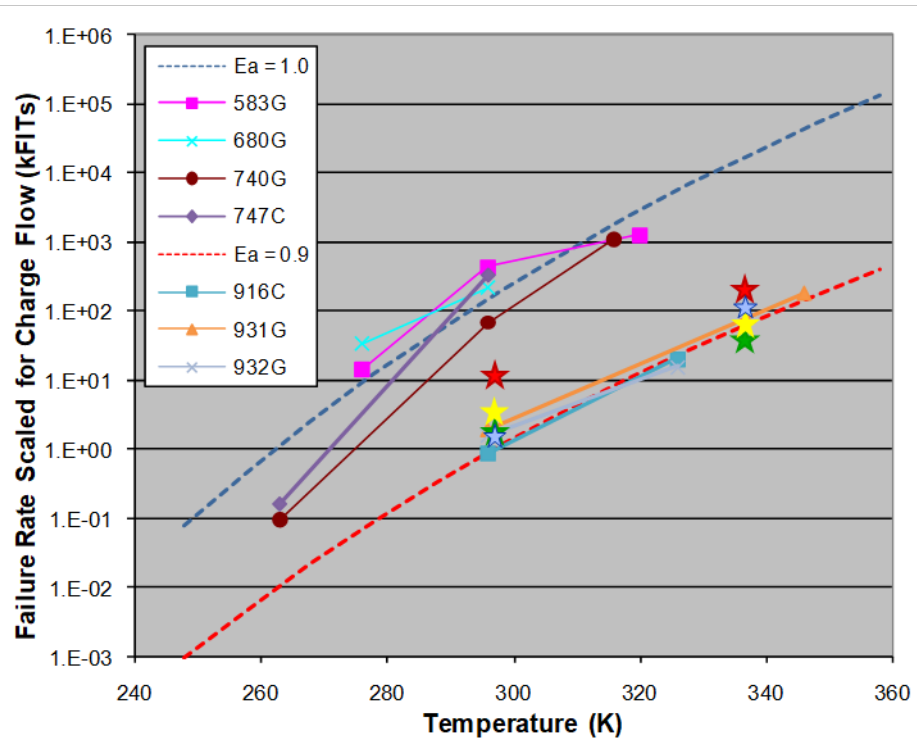
- **Failure mechanisms of Geiger-mode APDs**
 - DCR increase – primary “wear-out” mechanism for GmAPDs
 - Time to failure function of total amount of charge through APD and temperature
 - Dark current increase
 - Accompanies DCR increase during wear-out of APD
 - Electrical shorting
 - APDs that failed in this mode typically exhibited anomalous behavior in initial testing and can be screened for during assembly and burn-in
 - These failure mechanisms apply statistically to individual detector elements
- **Accelerated aging of APD arrays on fanout enables calculation of failure rates**
 - Increase charge flow through APDs to cause measurable failure rate
 - Scale to charge environment on ROIC to predict final FIT (failure in time) rates for detector pixels





Thermal Activation of Failure Rates

$$FailRate(I, T) \propto I \times \exp\left[\frac{-E_A}{kT}\right]$$

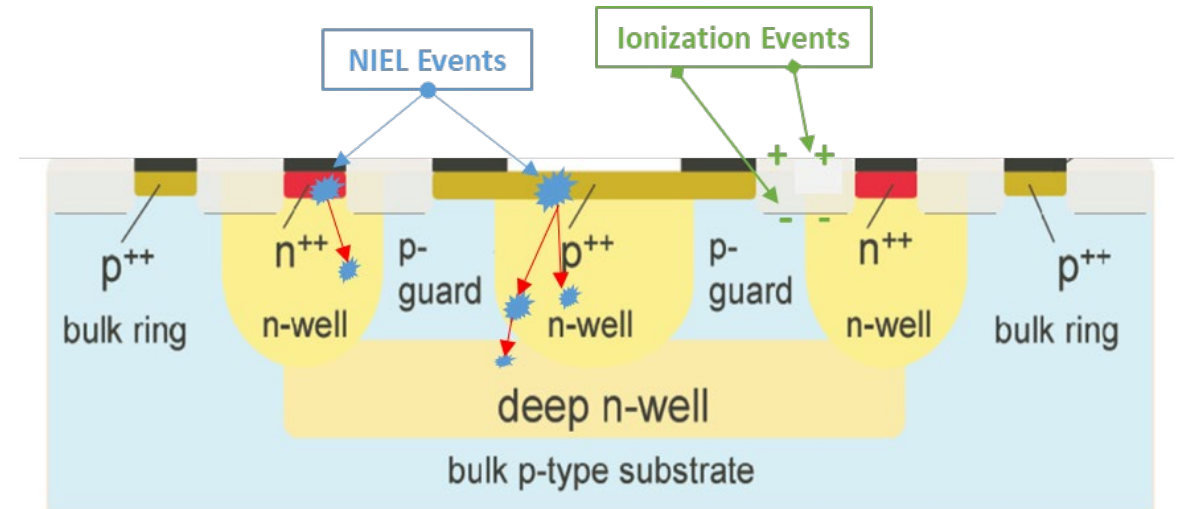
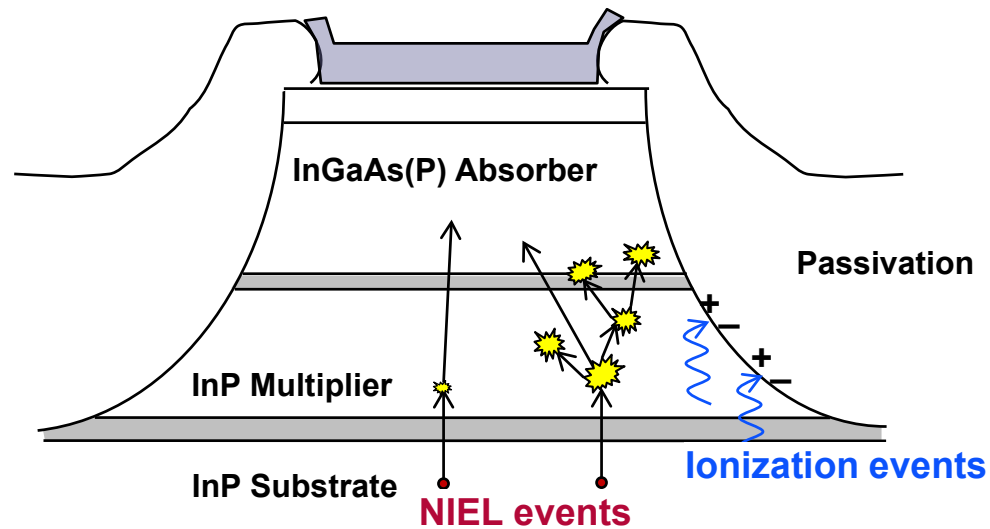


- Failure rate scaled for charge flow difference between fanout and ROIC (charge acceleration factors >100x)
- Failure rate measured as a function of temperature
- Failure rates for qualification lot (Blue stars) and flight lots (Green/Yellow stars) in agreement with past standard (good) fab lots
- Scaling to nominal operating temperatures (-10 to +10C) yields <200 FITs over this range of temperatures
 - MTBF >> mission time
 - 1kFITs: ~8000 years at 2hr/week ops
 - 200 FITs: ~40k years for this op-tempo



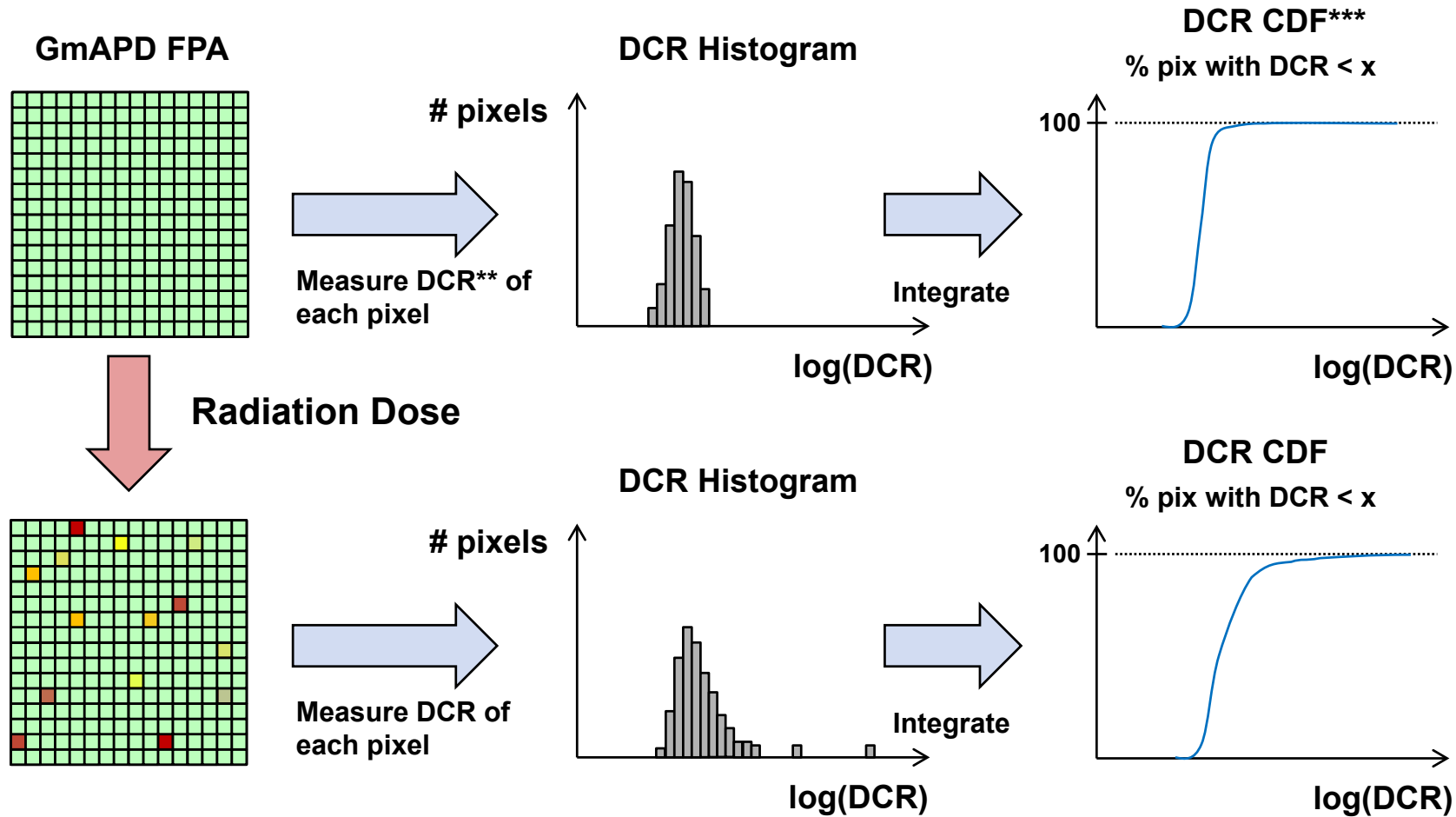
GmAPD radiation damage mechanisms

- Radiation Effects:
 - Ionizing – at the surface as charge is embedded in passivation layer
 - Non-ionizing (“NIEL”) – in the bulk, where displaced atoms generate electronic trap centers, leading to an increase in the dark count rate (DCR)
- Primary concern for *Geiger-mode* APDs is the increase in DCR due to displacement damage





Quantification of FPA Radiation Damage (DDD*)



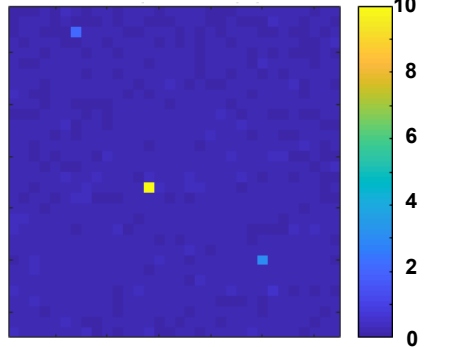
*DDD = Displacement Damage Dose, **DCR = Dark Count Rate, ***CDF = Cumulative Distribution Function



DDD*-Induced Change to DCR (InP)

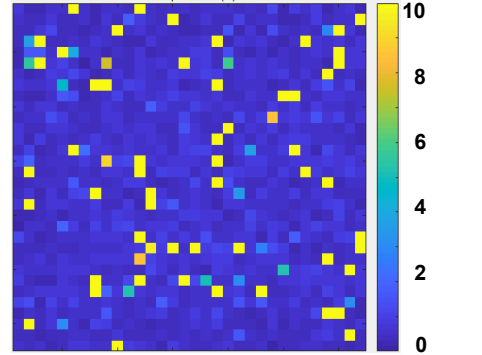
Pre-Dose Pixel DCR Map

Linear Scale (Hz) $\times 10^4$



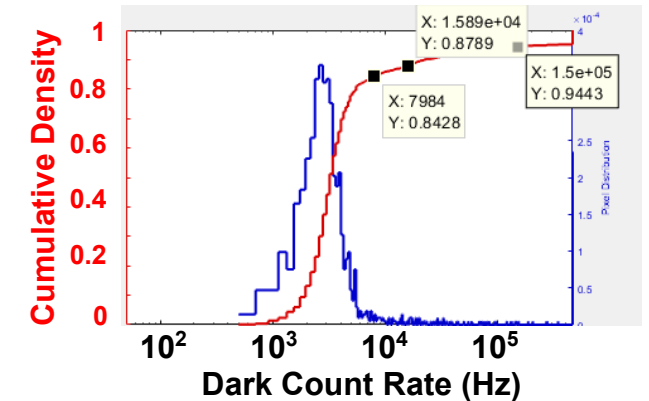
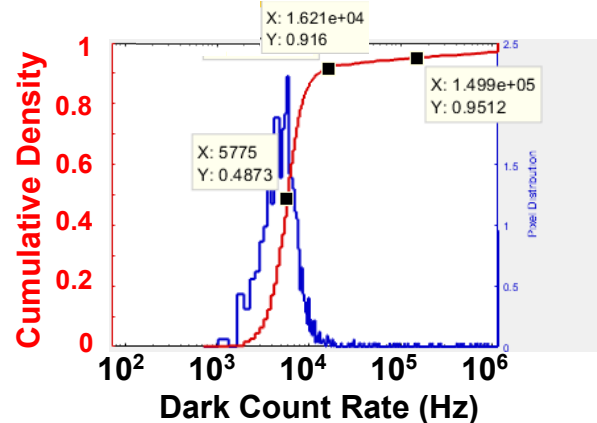
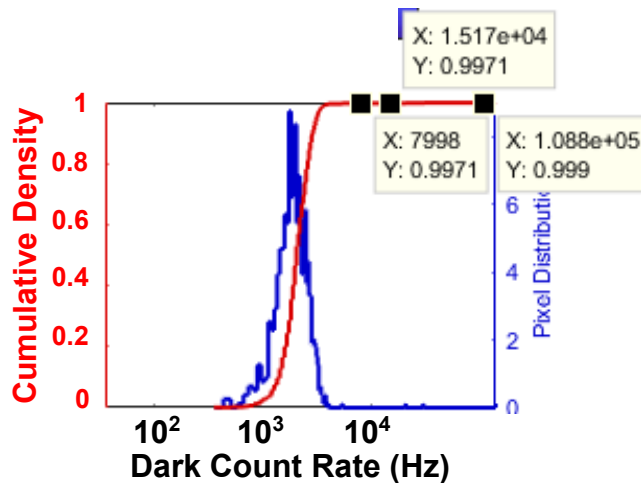
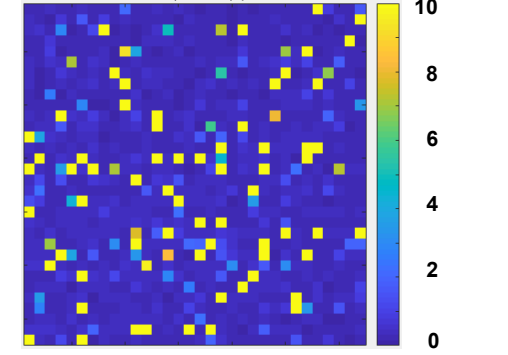
9.4e8 p+/cm² of 70MeV protons

Linear Scale (Hz) $\times 10^4$



2.3e9 p+/cm² of 70MeV protons

Linear Scale (Hz) $\times 10^4$

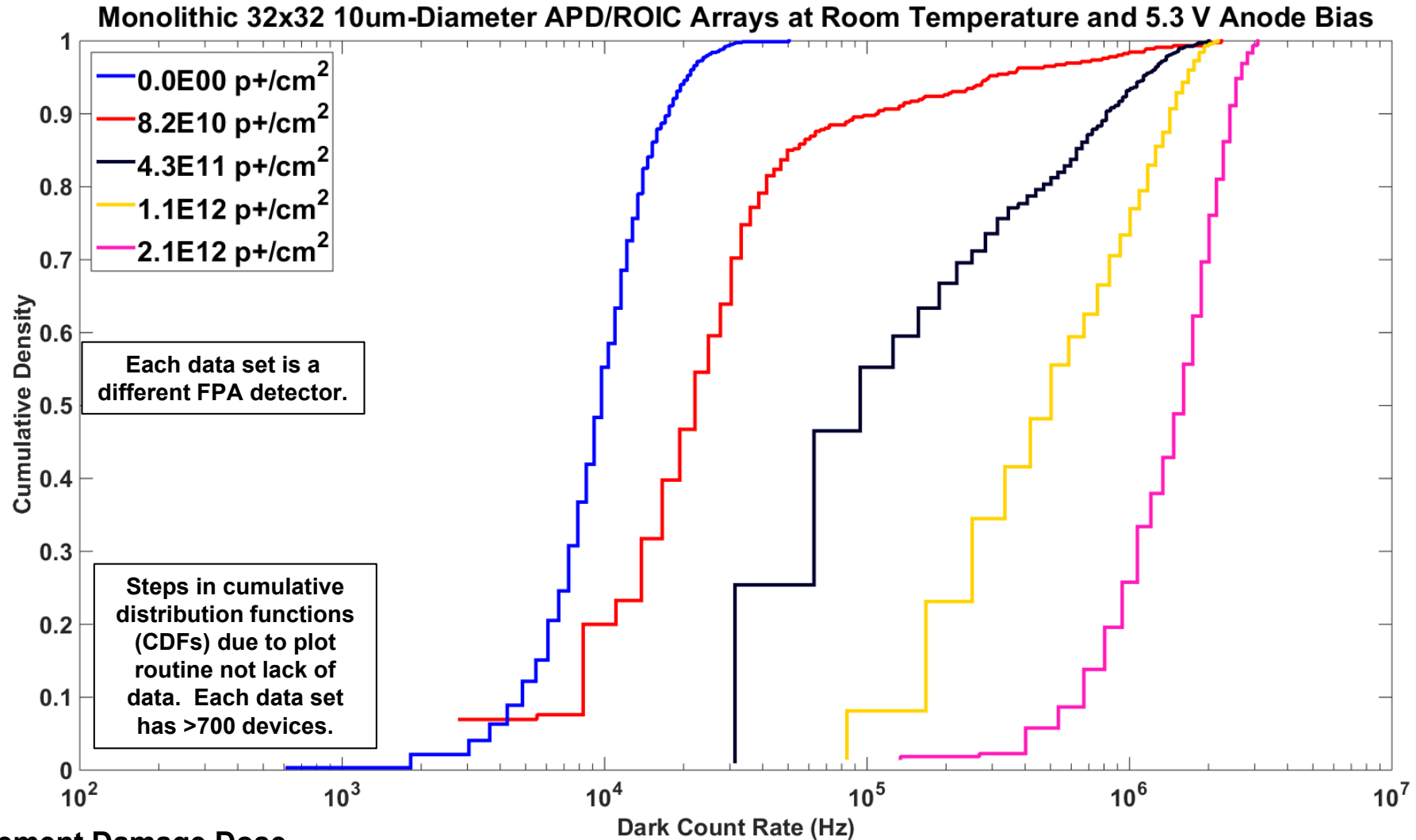


- Results are representative (i.e. not the same FPA for all 3 measurements)

*DDD = Displacement Damage Dose



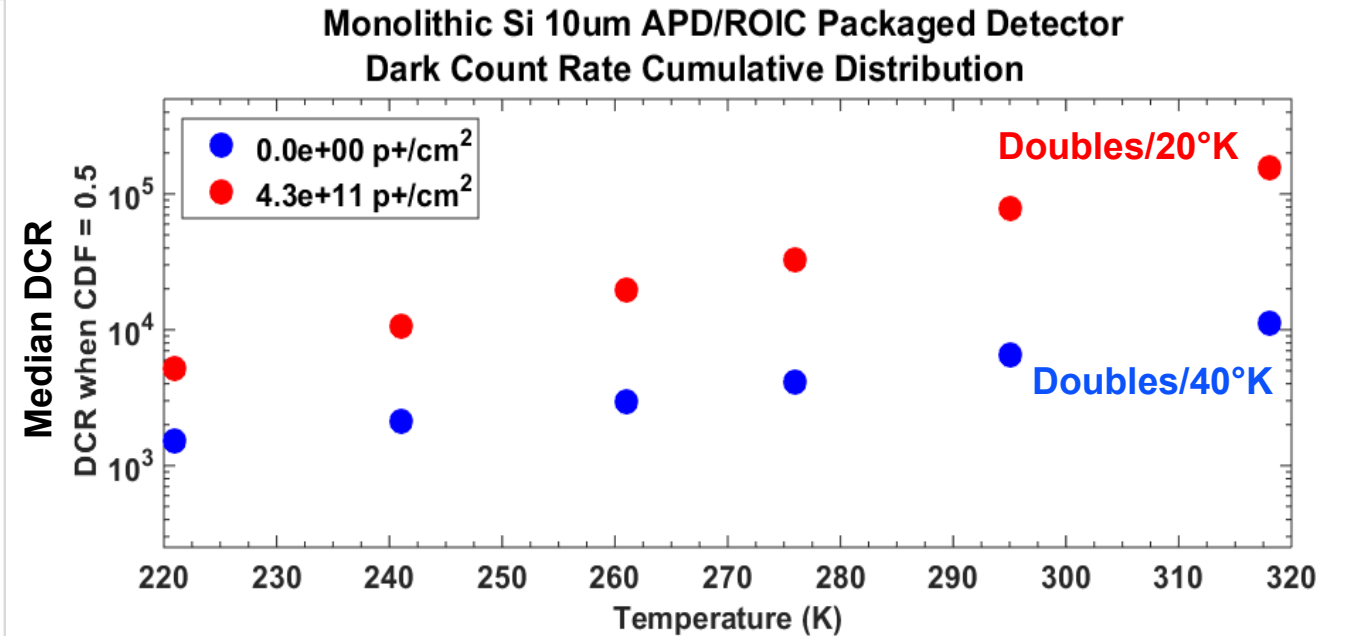
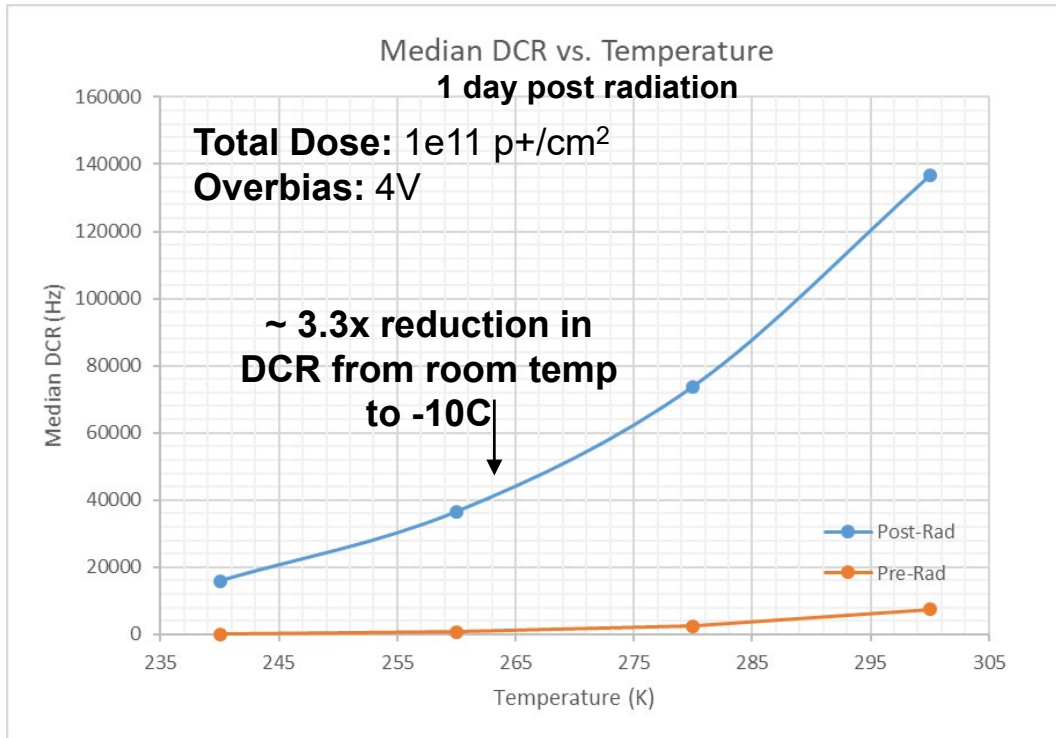
DDD*-Induced Change to DCR (Si)



*DDD = Displacement Damage Dose



DDD-Induced Median DCR vs. Temperature (Si)

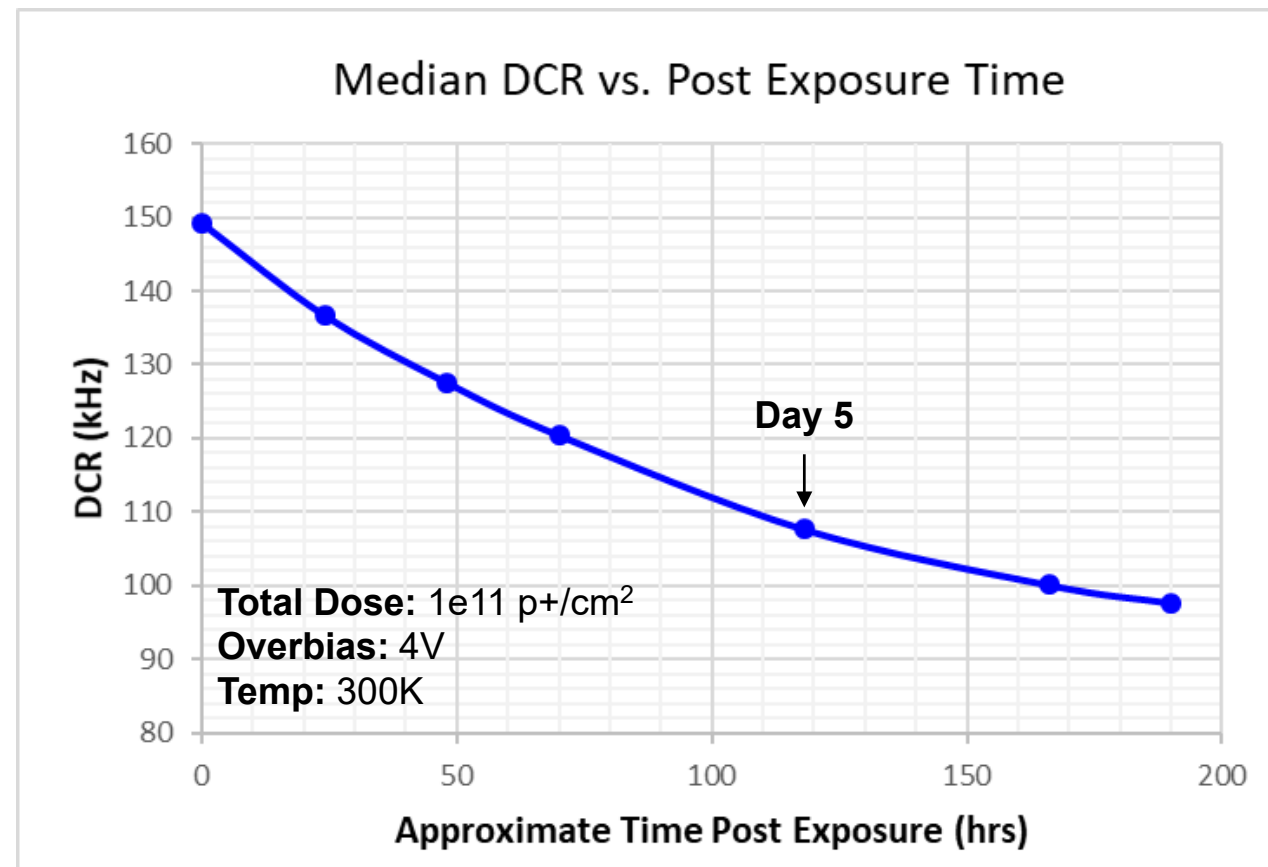


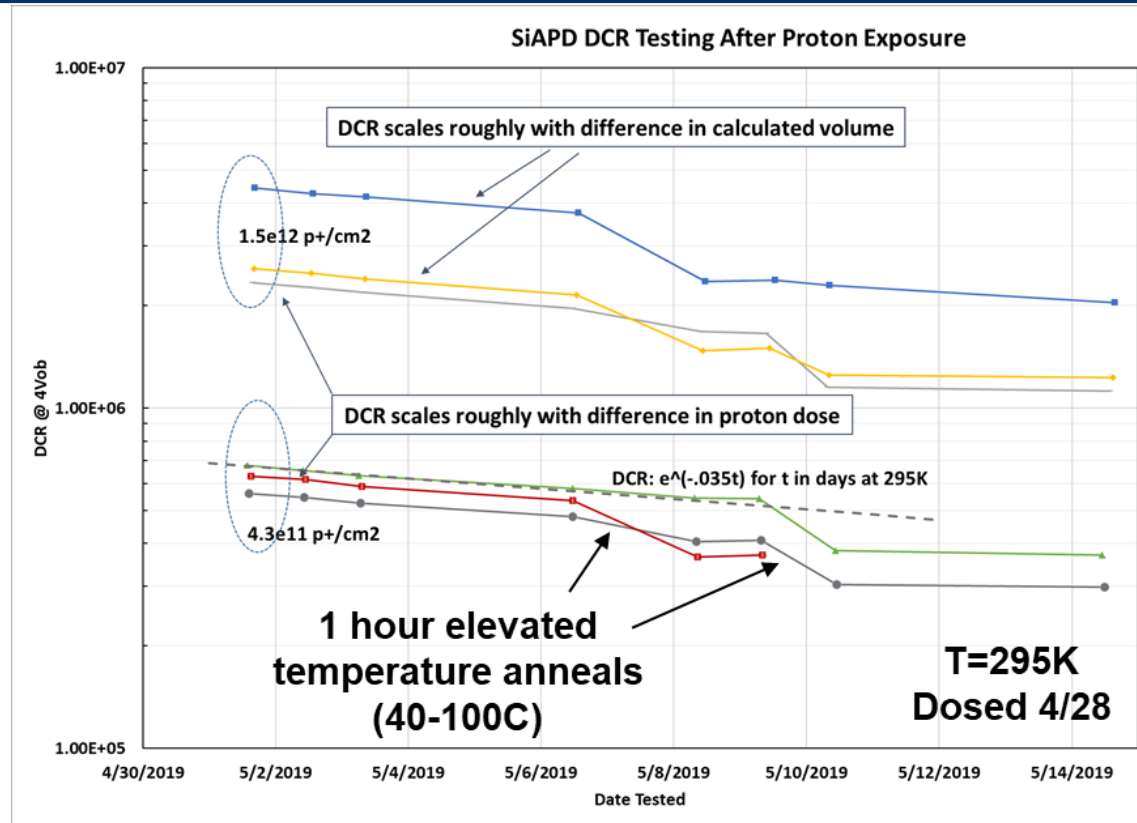
- Mean dark count rate shown as a function of temperature pre- and post-radiation
- Lower temperatures show overall benefit to reduction in dark count rate
- Analysis continues to identify cause of change in the slope for measured DCR



DDD-Induced Median DCR vs. Time (Si)

- DCR decreases by ~30% over 5 day period
- Scaling for temperature on Day 5: ~32kHz DCR @ -10C, ~41kHz DCR @ 0C

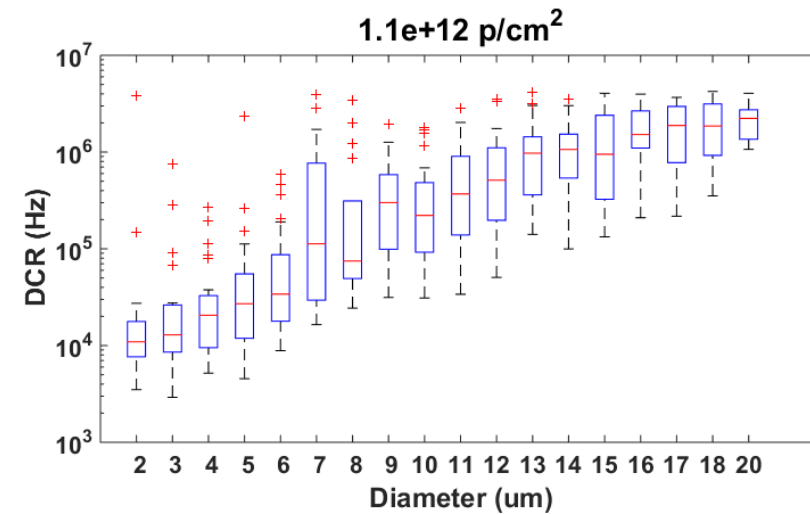
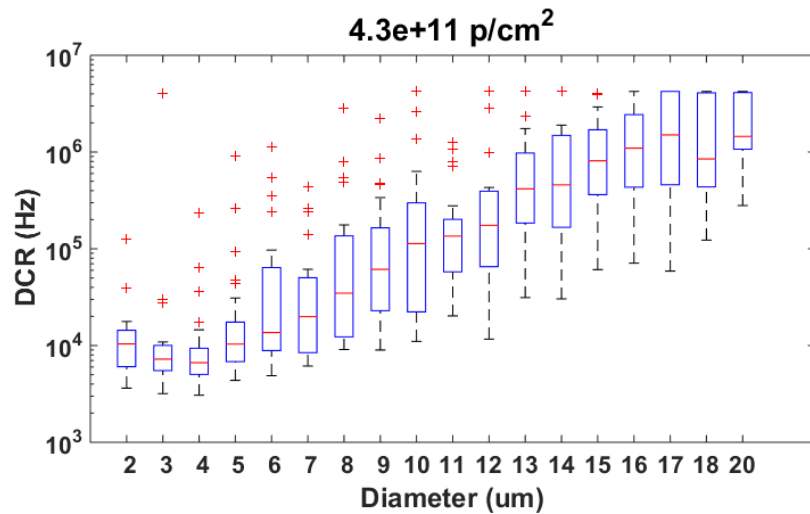
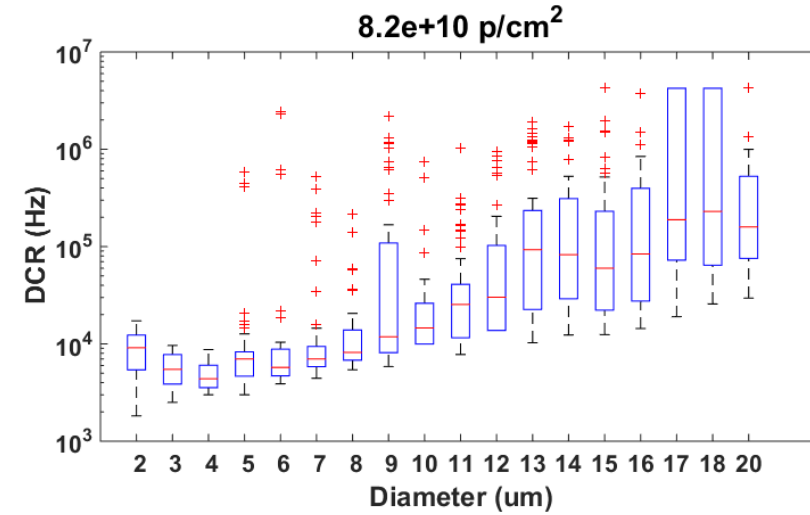
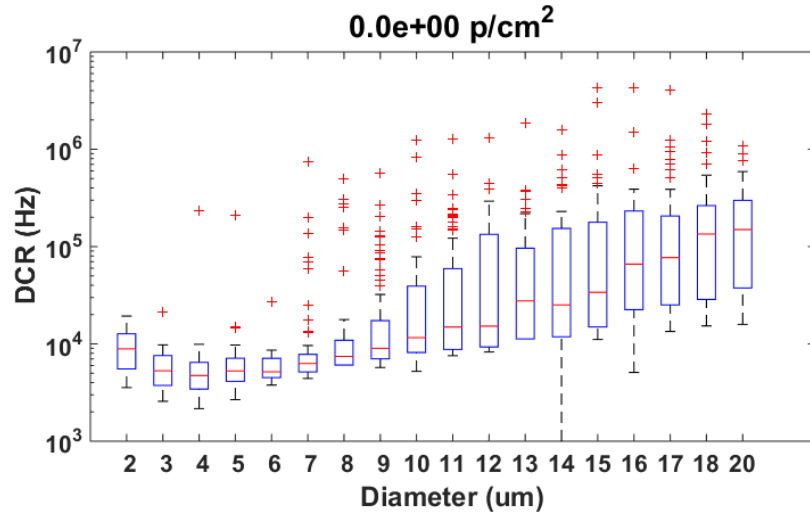




- Annealing at elevated temperatures shows more than one activation energy
 - $e^{(-0.031t)}$ to $e^{(-0.037t)}$, where t is days
- Elevated temperature anneals result in permanent decrease in DCR
 - 1-hour anneal at 100C ~ same as 290 hours at 23C



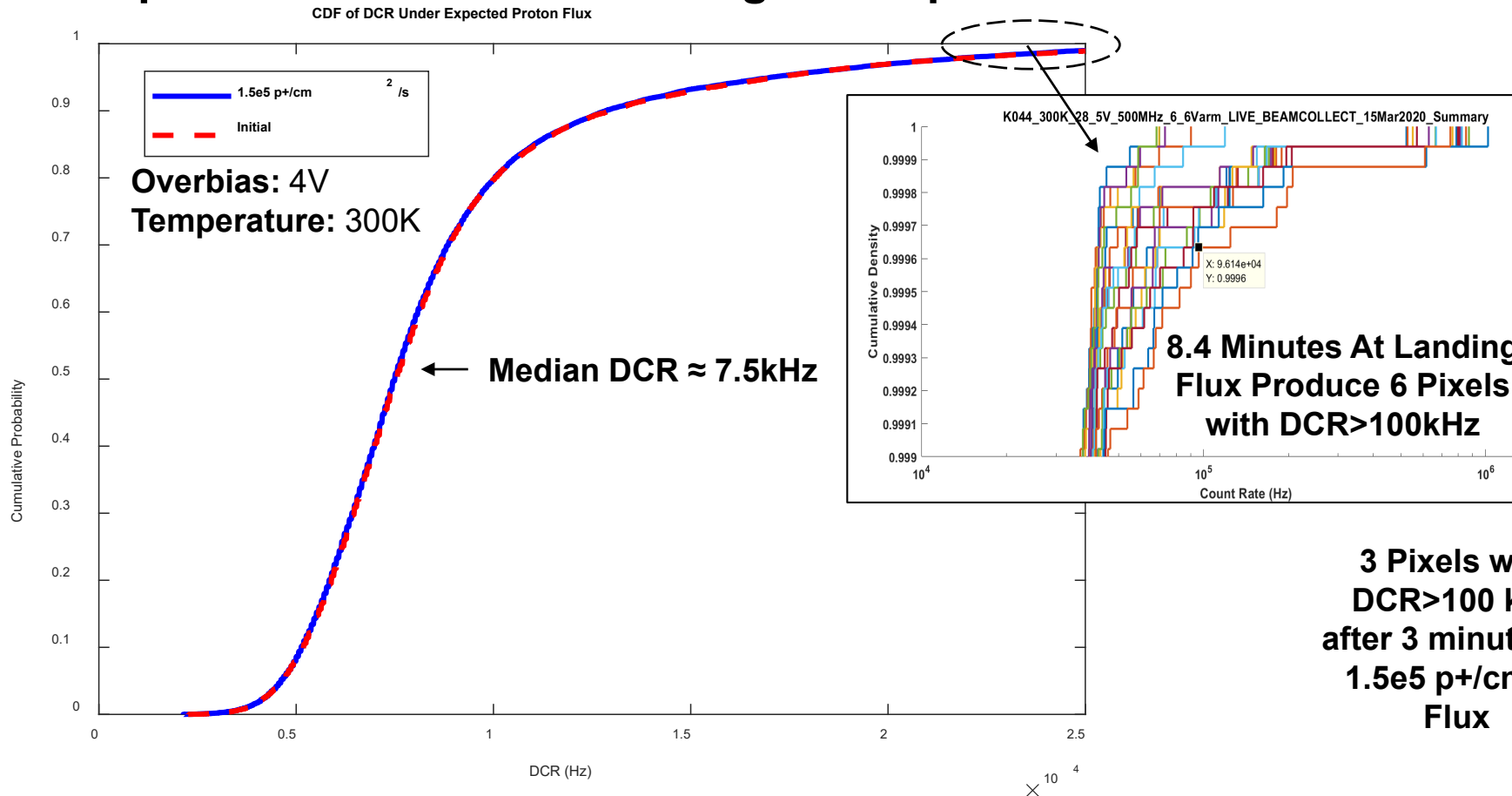
DDD-Induced DCR vs. SPAD Diameter (Si)



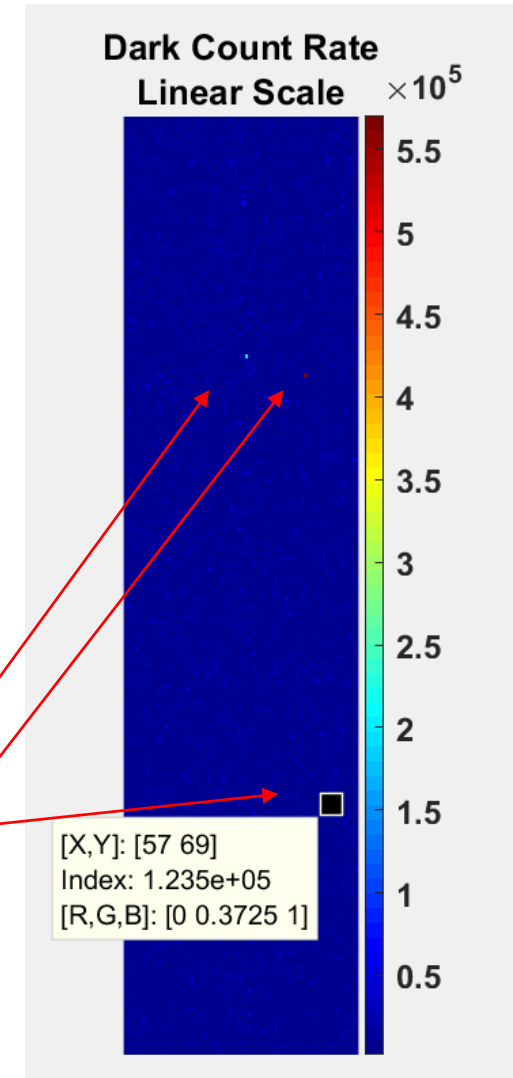


Live Testing with 70 MeV Protons (Si)

- No Change in median DCR under exposure to target proton flux of $1.5e5 \text{ p+}/\text{cm}^2/\text{s}$
- Proportional increase in # of high-DCR pixels



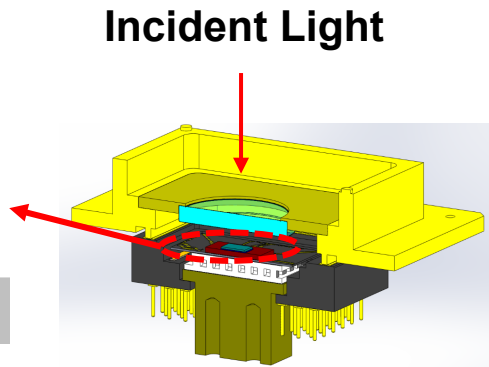
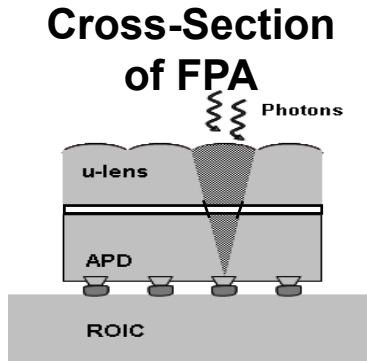
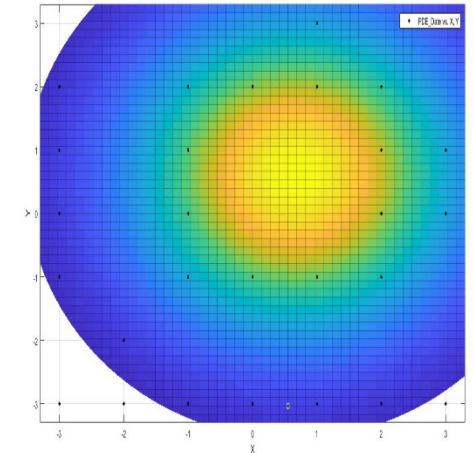
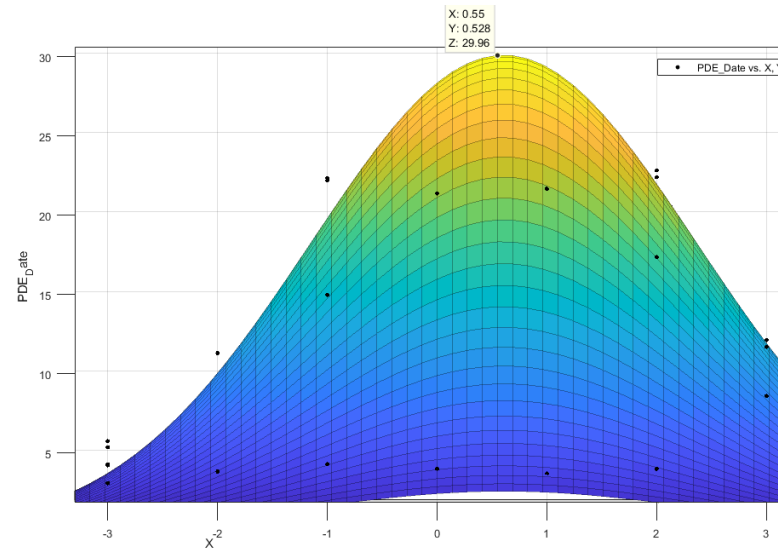
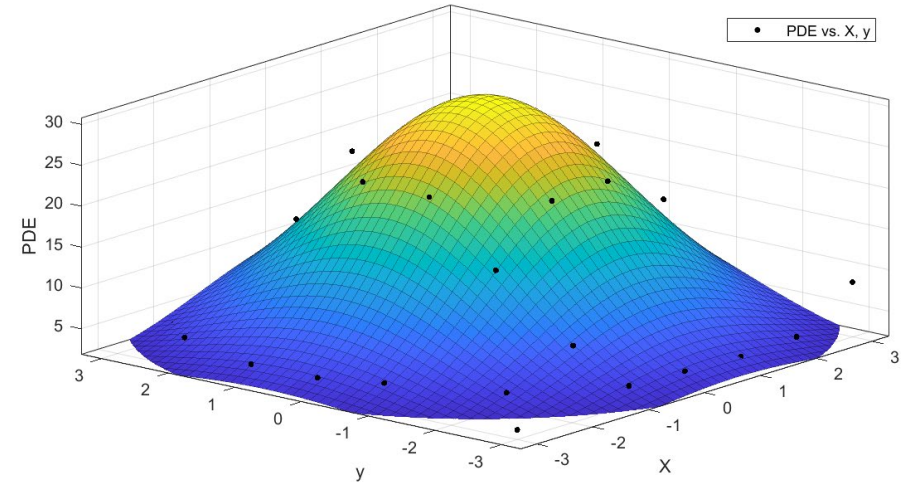
3 Pixels with DCR > 100 kHz after 3 minutes of $1.5e5 \text{ p+}/\text{cm}^2/\text{s}$ Flux





Microlens Coupling into Small SPADs

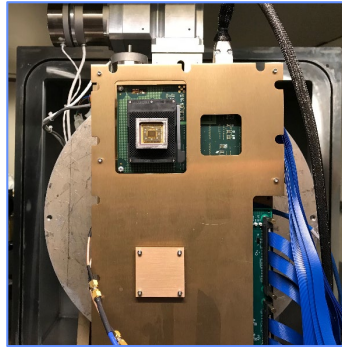
- Microlenses improve coupling of incident photons into active area
- Small diameter active area GmAPDs reduce sensitivity to displacement damage
 - Angle of acceptance determined by microlens design and APD diameter
 - MLAs are refractive GaP designs



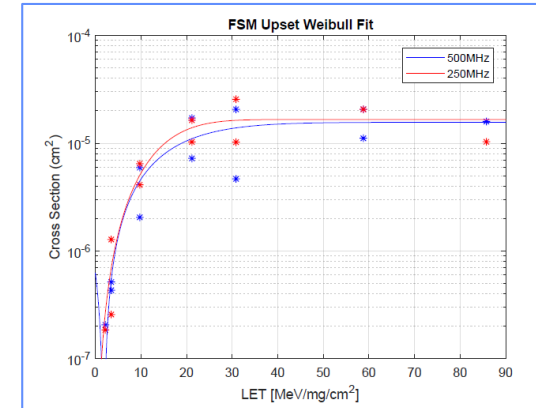


Single Event Effects in ROIC

Device in Test Chamber



Example Weibull Results



Upset Rate Estimates (Per Day)

Environment	Frequency	Fire Map	Timestamp	FSM	Counter
Nominal	500 MHz	2.030×10^{-4}	1.393×10^{-4}	3.119×10^{-5}	3.165×10^{-4}
Nominal	250 MHz	4.801×10^{-4}	1.471×10^{-3}	8.002×10^{-5}	9.482×10^{-5}
5-min. Worst Case	500 MHz	1.968	1.522	2.814×10^{-1}	2.405
5-min. Worst Case	250 MHz	3.788	3.830×10^2	3.921	1.031

- Heavy ion testing of ROICs to simulate SEE from space GCR/heavy ion environment
- Upset rates due to SEEs in ROIC determined to be low
 - Very low probability of upsets, even in worst case 5 minutes



Summary

- **MIT Lincoln Laboratory has partnered with the Jet Propulsion Laboratory to explore space-qualification GmAPD-based imagers**
- **In a space environment, the radiation effects primarily impacting GmAPD-based cameras are:**
 - **Displacement damage resulting in increased per-pixel DCR as a function of environment and lifetime**
 - **Single event effects impacting the custom readout integrated circuit (ROIC)**
- **A trade space of semiconductor, APD size, and temperature determine end-of-life performance and can be used to optimize performance for different requirements**